Cell Reports
Article

Crosstalk of Humoral and Cell-Cell Contact-Mediated Signals in Postnatal Body Growth

Xuefeng Jing,[1,4] Masayasu Miyajima,[2,4] Takahiro Sawada,[1,4] Qingfa Chen,[1] Keiji Iida,[3] Kenryo Furushima,[1] Daiki Arai,[1] Kazuo Chihara,[3] and Kazushige Sakaguchi[1,*]
[1]Department of Molecular Cell Biology and Molecular Medicine, Institute of Advanced Medicine
[2]Laboratory Animal Center
Wakayama Medical University, 811-1 Kimiidera, Wakayama 641-8509, Japan
[3]Division of Diabetes, Metabolism, and Endocrinology, Department of Internal Medicine, Kobe University Graduate School of Medicine, Kobe 650-0017, Japan
[4]These authors contributed equally to this work
*Correspondence: ksaka@wakayama-med.ac.jp
http://dx.doi.org/10.1016/j.celrep.2012.08.021

SUMMARY

The growth hormone (GH)–insulin-like growth factor 1 (IGF1) axis mediates postnatal body growth. The GH receptor has been regarded as the sole receptor that mediates the Janus kinase 2 (JAK2)/signal transducers and activators of the transcription 5B (STAT5B) signal toward IGF1 synthesis. Here, we report a signaling pathway that regulates postnatal body growth through EphA4, a member of the Eph family of receptor tyrosine kinases and a mediator of the cell-cell contact-mediated signaling. EphA4 forms a complex with the GH receptor, JAK2, and STAT5B and enhances *Igf1* expression predominantly via the JAK2-dependent pathway, with some direct effect on STAT5B. Mice with a defective *Epha4* gene have a gene dose-dependent short stature and low plasma IGF1 levels. *Igf1* messenger RNA (mRNA) in the liver and many other tissues was also significantly reduced in *Epha4*-knockout mice, whereas pituitary *Gh* mRNA and plasma GH levels were not. These findings suggest that the local cell-cell contact-mediated ephrin/EphA4 signal is as important as the humoral GH signal in IGF1 synthesis and body size determination.

INTRODUCTION

Growth hormone receptor (GHR) is present as a preformed dimer in hepatocytes and other cells. Binding of growth hormone (GH) triggers a conformational change in the extracellular domain that initiates downstream signaling (Birzniece et al., 2009; Cunningham et al., 1991; Rowlinson et al., 1998). In common with other cytokine receptors, GHR is devoid of enzymatic activity, and signal transduction is mediated by Janus kinase 2 (JAK2) (Pilecka et al., 2007). On binding of GH to the receptor, JAK2 is catalytically activated by transphosphorylation. Intracellular GH signaling appears to comprise three main pathways: the signal transducers and activators of transcription (STAT) pathway, the mitogen-activated protein kinase (MAPK) pathway, and the phosphoinositide 3 (PI-3) kinase pathway (Piwien-Pilipuk et al., 2002). Although these three pathways are activated by JAK2 transphosphorylation, the JAK-STAT pathway is regarded as the major effector of GHR signaling and is required for transcriptional regulation of insulin-like growth factor 1 (IGF1) in hepatic cells as well as locally in tissues (Kofoed et al., 2003). Among several STAT proteins, STAT5B is directly linked to the transcriptional regulation of IGF1 (Kofoed et al., 2003). Circulating IGF1 is produced predominantly in hepatocytes (Sjögren et al., 1999; Yakar et al., 1999) and is present as a ternary complex with IGF-binding protein 3 (IGFBP3) and acid-labile subunit (IGFALS) (Domené et al., 2004). The ternary complex slows the clearance of IGF1. Changes in the expression of IGFBP3 and IGFALS play an important role in modulating the growth-promoting actions of circulating IGF1, but not of local IGF1. IGFALS is produced by hepatocytes in a GH-dependent manner. In contrast, IGFBP3 is produced primarily by hepatic endothelial and Kupffer cells in the liver, although it is widely expressed in many tissues and the mechanism of IGFBP3 transcriptional regulation is not clearly defined (Binoux, 1997).

The GH-IGF1 axis is a major mediator of postnatal body growth. Defects in any of the molecules related to the GH-IGF1 axis result in short stature (Walenkamp and Wit, 2006; Woods, 2007). There are currently four known genetic causes of GH insensitivity (Woods, 2007). Homozygous mutation of the *GHR* gene is a cause of short stature (Laron syndrome), which was originally reported in patients with the classical clinical features of congenital GH deficiency and an elevated circulating GH level (Amselem et al., 1989; Godowski et al., 1989; Laron et al., 1966). Homozygous mutation of *STAT5B* was subsequently identified as causing phenotypes similar to severe GHR deficiency (Kofoed et al., 2003). Patients with *STAT5B* mutation have low levels of IGF1 and IGFBP3 and do not respond to exogenous GH administration. These genetic defects are associated with normal to mildly reduced birth weight. In contrast, *IGF1* gene deficiency causes substantial prenatal growth retardation with elevated levels of GH and normal levels of IGFBP3 and IGFALS (Woods et al., 1996). Patients with homozygous mutation of the *IGFALS* gene exhibit only a mild degree of growth retardation and have elevated GH secretion and very low circulating levels of IGF1

and IGFBP3 (Domené et al., 2004). Despite this knowledge, there appear to be many patients with short stature who have no clear molecular defects in these molecules.

Ephrin receptors (Ephs) belong to a superfamily of receptor tyrosine kinases classified into two subclasses, A and B, by their ligand-binding specificity (Kullander and Klein, 2002). The EphA receptors, with exception of EphA4, bind to ephrin-As, which are anchored to the cell membrane via a glycosylphosphatidylinositol linkage. The EphB receptors bind to ephrin-Bs, which have a transmembrane domain and a short cytoplasmic domain. EphA4 binds not only to all ephrin-As, but also to ephrin-B2 and ephrin-B3. Ephrin-Eph signaling mediates a number of functions, including classical repulsive axon guidance, boundary formation, cell migration, and proliferation via forward signaling from ephrin to Eph and reverse signaling from Eph to ephrin (Pasquale, 2008). Some signals are stimulatory, whereas others are inhibitory. Recent reports suggest that Eph receptors also regulate angiogenesis in embryonic and adult tissues (Zhang and Hughes, 2006). We have previously reported their interaction with fibroblast growth factor receptors (FGFRs) and enhancement of the canonical fibroblast growth factor signaling pathway (Sawada et al., 2010; Yokote et al., 2005). However, a complete view of the biologic functions of Ephs and ephrins has yet to be clarified.

Here, we report functions of EphA4 in JAK2-dependent and -independent STAT5B activation, leading to enhanced synthesis of IGF1. Mice defective in the *Epha4* gene showed moderate to severe short stature and low expression of *Igf1* in the liver and many other tissues. Our findings suggest that the ephrin/EphA4 and GH/GH receptor signal systems function synergistically in the production of IGF1 in multiple tissues and contribute to postnatal body and organ growth.

RESULTS

Short Stature in *Epha4*-Knockout Mice

Short stature is one of the main clinical phenotypes caused by derangement of the GH-IGF1 axis. Several genetic abnormalities have been reported among members of this signal transduction pathway, including genes for GH, GHR, STAT5B, and IGF1 (Woods, 2007). We identified short stature in $Epha4^{+/-}$ and $Epha4^{-/-}$ mice (Figure 1A). Prenatal body weight was similar among the three genotypes: $Epha4^{+/+}$, $Epha4^{+/-}$, and $Epha4^{-/-}$. However, $Epha4^{+/-}$ and $Epha4^{-/-}$ mice showed significant growth retardation compared with wild-type (WT) mice after birth. The growth retardation of $Epha4^{+/-}$ mice was milder than that of $Epha4^{-/-}$ mice. This growth deficiency was clearly present, not only in body size, but also in the skeletal system and in organs, such as the liver (Figures 1B and 1C; Table S1). These findings suggested that EphA4 might be a determinant of body size after birth.

Generalized Shrinkage of Epiphyseal Growth Plates in *Epha4*-Knockout Mice

Longitudinal growth retardation is caused by defective development of epiphyseal growth plates. As stated earlier, EphA4 interacts with FGFRs and enhances signaling via the canonical FGFR signaling pathway (Sawada et al., 2010; Yokote et al., 2005). Therefore we examined tibial epiphyseal growth plates to determine if there was shrinkage or elongation of the prehypertrophic chondrocytes, as seen in mice with mutated *Fgfr3* (Naski et al., 1998). Hematoxylin-eosin staining and in situ hybridization of *Col2a1* (collagen 2a1) messenger RNA (mRNA) of epiphyseal sections revealed severe shrinkage of all layers of growth plates in $Epha4^{-/-}$ mice (Figure 1D). This was contrary to the finding expected from inactivation of FGFR3 signaling, which shows elongation of longitudinal bones (Ornitz, 2001).

Food Intake and Plasma Levels of GH, Thyroxine, and Corticosterone Are Not Determinants of Small Body Size in *Epha4*-Knockout Mice

Malnutrition is a major cause of growth retardation. To determine if *Epha4*-targeted mice had problems with food intake, we examined daily food intake in adult mice. Weight-adjusted food intake in $Epha4^{-/-}$ and $Epha4^{+/-}$ mice was not reduced compared with WT mice (Table S1), suggesting that the amount of food intake is not a determinant of small body size in EphA4-deficient mice. Body length was also significantly different between $Epha4^{+/+}$ and $Epha4^{-/-}$ mice in both sexes (Table S1). *Epha4* knockout did not significantly alter plasma levels of GH, thyroxine, or corticosterone that might influence body size (Figure 1E).

Secretion of GH is reported to be pulsatile, such that the plasma GH level at a given time point might be misleading with respect to the state of GH production (MacLeod et al., 1991). To examine GH expression in the pituitary, we quantified the amount of *Gh* mRNA by real-time RT-PCR. Quantities were corrected for the amount of *18S* ribosomal RNA (rRNA) amplified, as reported (Iida et al., 2004). The *Gh* mRNA/*18S* rRNA values were not significantly different among the three *Epha4* genotypes in each sex or between sexes (Figure 1F).

Plasma Levels of IGF1, IGFALS, and IGFBP3 Are Reduced in *Epha4*-Knockout Mice

Plasma levels of IGF1, IGFALS, and IGFBP3 are important parameters for the function of the GH-IGF1 axis. Levels of these proteins were significantly less in $Epha4^{-/-}$ mice compared with WT mice in both sexes (Figure 2A). The plasma IGF1 level of female $Epha4^{-/-}$ mice was 49.7% that of WT mice, and that of male $Epha4^{-/-}$ mice was 36.5% that of WT mice. The plasma IGFALS level of female $Epha4^{-/-}$ mice was also reduced to 53.2% that of the control, while that of male $Epha4^{-/-}$ mice was 57.2% that of WT mice (Figure 2B). The IGFBP3 level of female $Epha4^{-/-}$ mice was 34.1% that of WT mice, and that of male $Epha4^{-/-}$ mice was 60.3% that of WT mice (Figure 2C). The low levels of these three factors in the presence of normal plasma GH level suggested that the GH-IGF1 axis in the liver is impaired because of deletion of the *Epha4* gene. The smaller liver size of $Epha4^{-/-}$ mice (Figure 1C; Table S1) might imply functional resistance at the level of GHR or IGF1 receptor (IGF1R), since EphA4, GHR, and IGF1R are all expressed in the same cell surface compartment.

Epha4 Knockout Reduces Hepatic mRNA Expression of *Igf1* and *Igfals*, but Not of *Igfbp3*, *Ghr*, or *Igf1r*

Given that approximately 75% of plasma IGF1 is produced in the liver in response to GH, we examined the hepatic expression of

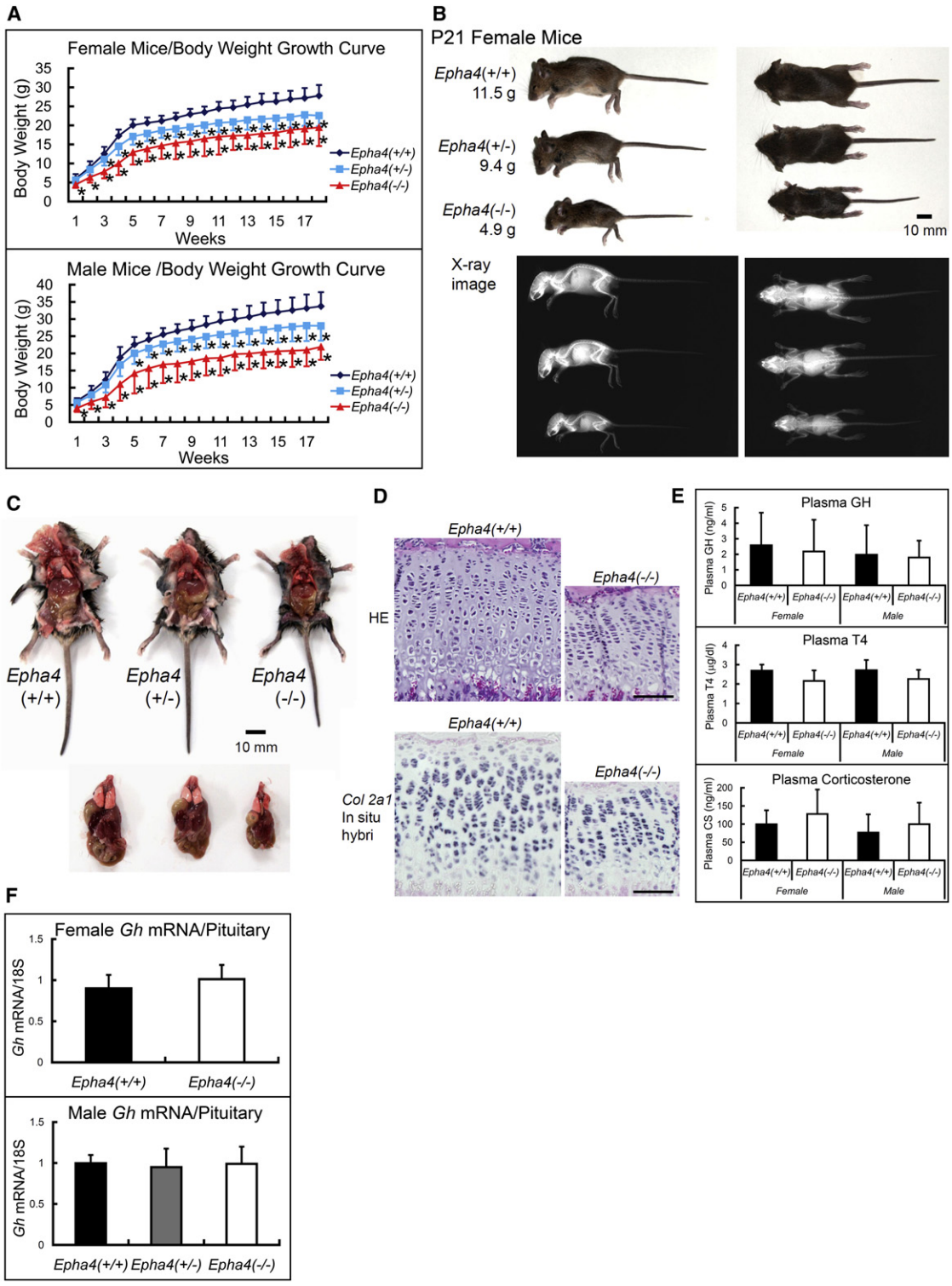

Figure 1. Body Size of *Epha4* Genetically Engineered Mice

(A) Growth curves of *Epha4*-targeted mice. Body weights of WT (female, n = 14; male, n = 20), $Epha4^{+/-}$ (female, n = 50; male, n = 50) and $Epha4^{-/-}$ (female, n = 22; male, n = 16) mice were measured every week. Data are presented as mean ± SD values. *p < 0.01 compared with WT mice.

(B) Typical body and soft X-ray images of 3-week-old sibling female mice with genotypes of $Epha4^{+/+}$, $Epha4^{+/-}$, and $Epha4^{-/-}$.

(C) Organs of 3-week-old female mice with genotypes of $Epha4^{+/+}$, $Epha4^{+/-}$, and $Epha4^{-/-}$ (upper panels). The abdominal and thoracic organs are viewed from the back side (lower panels).

Igf1 mRNA (Figure 2D). Both male and female *Epha4*$^{-/-}$ mice showed significantly less *Igf1* mRNA expression compared with WT mice. IGFALS, like IGF1, is produced by hepatocytes, and its transcription depends on the level of GH (Binoux, 1997). In our study, the *Igfals* mRNA level was also significantly reduced in *Epha4*$^{-/-}$ mice of both sexes compared with the WT (Figure 2E). In contrast, expression of *Igfbp3* mRNA, synthesized primarily by Kupffer cells and sinusoidal endothelial cells in the liver, is not directly regulated by the GH signal, and the ternary complex of IGF1-IGFBP3-IGFALS plays an important role in the clearance of its components (Binoux, 1997). When hepatic *Igfbp3* mRNA was quantified, the expression was similar, regardless of the expression of *Epha4* in either sex (Figure 2F), suggesting that the low plasma IGFBP3 levels in *Epha4*$^{-/-}$ mice are due to rapid clearance from the circulation caused by the low levels of plasma IGF1 and IGFALS. These findings support the idea that the function of GH on hepatocytes mediated by GHR is impaired in *Epha4*$^{-/-}$ mice. We demonstrated colocalization of EphA4 and GHR in HepG2 cells, a hepatoma cell line, using immunocytochemistry followed by detection with a confocal microscope (Figure S1).

We also examined the expression of liver *Ghr* and *Igf1r* mRNA to obtain the whole picture of the GH-IGF1 axis in *Epha4*$^{-/-}$ mice. The expression of mRNA was unchanged in *Epha4*$^{-/-}$ mice compared with the WT (Figures 2G and 2H). To examine the significance of *Epha4* gene deletion in the liver, we tested expression of all *Epha* and *Efn* members in the liver and found that multiple *Epha* members (*a1*, *a2*, *a3*, *a4*, and *a7*), *Efna* members (*a1, a2, a4*, and *a5*), and *Efnb* members (*b1* and *b2*) were expressed (Figure 2I). Among the ephrins expressed in the liver, ephrin-A1, -A2, -A4, -A5, and -B2 are currently regarded as ligands for EphA4.

Epha4 Knockout Reduces Extrahepatic mRNA Expression of *Igf1*, but Not of *Ghr* or *Igf1r*

We quantified *Igf1*, *Ghr*, and *Igf1r* mRNA expression levels in various tissues of WT and *Epha4*$^{-/-}$ mice. *Epha4*$^{-/-}$ mice of either sex showed significantly lower expression levels of *Igf1* mRNA than WT mice in heart, lung, spleen, stomach, small intestine, colon, skin, and muscle (Figure 3A). However, cerebrum and kidney showed no significant difference in *Igf1* mRNA expression. In contrast, mRNAs for *Ghr* and *Igf1r* were expressed at similar levels in all of these tissues in WT and *Epha4*$^{-/-}$ mice (Figures 3B and 3C). In addition, *Epha4* was expressed in all tissues examined in WT mice (Figure 3D).

Interaction of EphA4, GHR, and JAK2

EphA4 belongs to a family of receptor tyrosine kinases located at the cell surface, where GHRs are also present. There have been no reports of interaction between these two receptors. Therefore, we examined their potential interaction in HEK293T cells, in which EphA4, GHR, and JAK2 were overexpressed (Figure 4A). The three proteins bound directly to each other, forming a ternary complex.

We also demonstrated that these molecules, which are expressed endogenously in fibroblasts, form a complex following ligand stimulation. Knockdown of *Ghr* by small hairpin RNA (shRNA) in fibroblasts (see Figure S2 for *Ghr* mRNA reduction by more than 70%) reduced the amount of endogenous EphA4 and JAK2 coimmunoprecipitated with GHR (Figure 4B, left panels). As shown in the cells from which *Epha4* or *Jak2* were genetically deleted, we detected binding of GHR-EphA4 and GHR-JAK2 (Figure 4B, middle panels). However, the EphA4-JAK2 binding was not clearly detectable in *Ghr*$^{-/-}$ cells (data not shown). Interestingly, endogenous STAT5B also bound to the complex, and EphA4-STAT5B binding was present in the absence of GHR. Stimulation with ligands completely abolished the EphA4-STAT5B binding in *Ghr*$^{-/-}$ cells (Figure 4B, right panels), suggesting the release of STAT5B from activated EphA4. In addition to these coimmunoprecipitation studies to detect molecular interactions, we have shown immunocytochemical colocalization of GHR and EphA4 molecules on the cell surface in the HepG2 hepatoma cell line (Figure S1).

Effect of EphA4 on Signals Downstream of GHR in Fibroblasts

We cultured fibroblasts from mice in which the *Epha4* or *Jak2* gene was genetically knocked out and studied receptor binding and signal transduction in cells with or without retrovirus-based expression rescue of the respective gene. Notably, fibroblasts derived from WT mice expressed many of the *Epha* members (*a1*, *a2*, *a3*, *a4*, *a5*, *a7*, and *a8*), *Ephb* members (*b1, b2, b3, b4*, and *b6*), *Efna* members (*a1, a2, a3, a4*, and *a5*) and *Efnb* members (*b1, b2*, and *b3*). Knockout or rescue of *Epha4* did not alter mRNA expression levels of other members of the *Eph* family or their ligands (Figure 4C).

Fibroblasts from *Epha4*$^{-/-}$ mice showed a decreased response to GH stimulation in the phosphorylation of tyrosines in GHR and JAK2, and the response was augmented by rescued expression of *Epha4* (Figure 4D). However, we obtained the most prominent sustained phosphorylation of GHR/JAK2/STAT5B in cells preincubated with ephrin-A1 (500 ng/ml) for 45 min before addition of GH (Figure 4E). Interestingly, ephrin ligand–stimulated enhancement of STAT5B phosphorylation in nonrescued cells was similar to that in EphA4-rescued cells, suggesting that EphAs other than EphA4 were also able to augment the function of ligand-stimulated GHR following strong activation by ephrin-A1. Binding of EphA4 to the GHR/JAK2 complex was clearly demonstrated by coimmunoprecipitation studies with anti-GHR or anti-JAK2 antibody (Figure 4E). The binding appeared to be strengthened by activation of EphA4 with ephrin-A1. In addition, ephrin-A1 stimulation alone induced rapid

(D) Hematoxylin-eosin staining and collagen type 2a1 (*Col2a1*) mRNA in situ hybridization of epiphyseal growth plates of tibiae from 3-week-old female *Epha4*$^{+/+}$ and *Epha4*$^{-/-}$ mice. Scale bar, 100 μm.

(E) Plasma levels of GH, thyroxine (T4), and corticosterone in *Epha4*$^{+/+}$ and *Epha4*$^{-/-}$ mice. Blood was drawn early in the morning, and hormone levels were measured as described.

(F) Pituitary *Gh* mRNA expression. Adult mice 4 months of age or older were used. Pituitary *Gh* mRNA relative to *18S* rRNA was measured as described.

Data in (E) and (F) are presented as mean ± SD values of six independent samples. See also Table S1 for additional information.

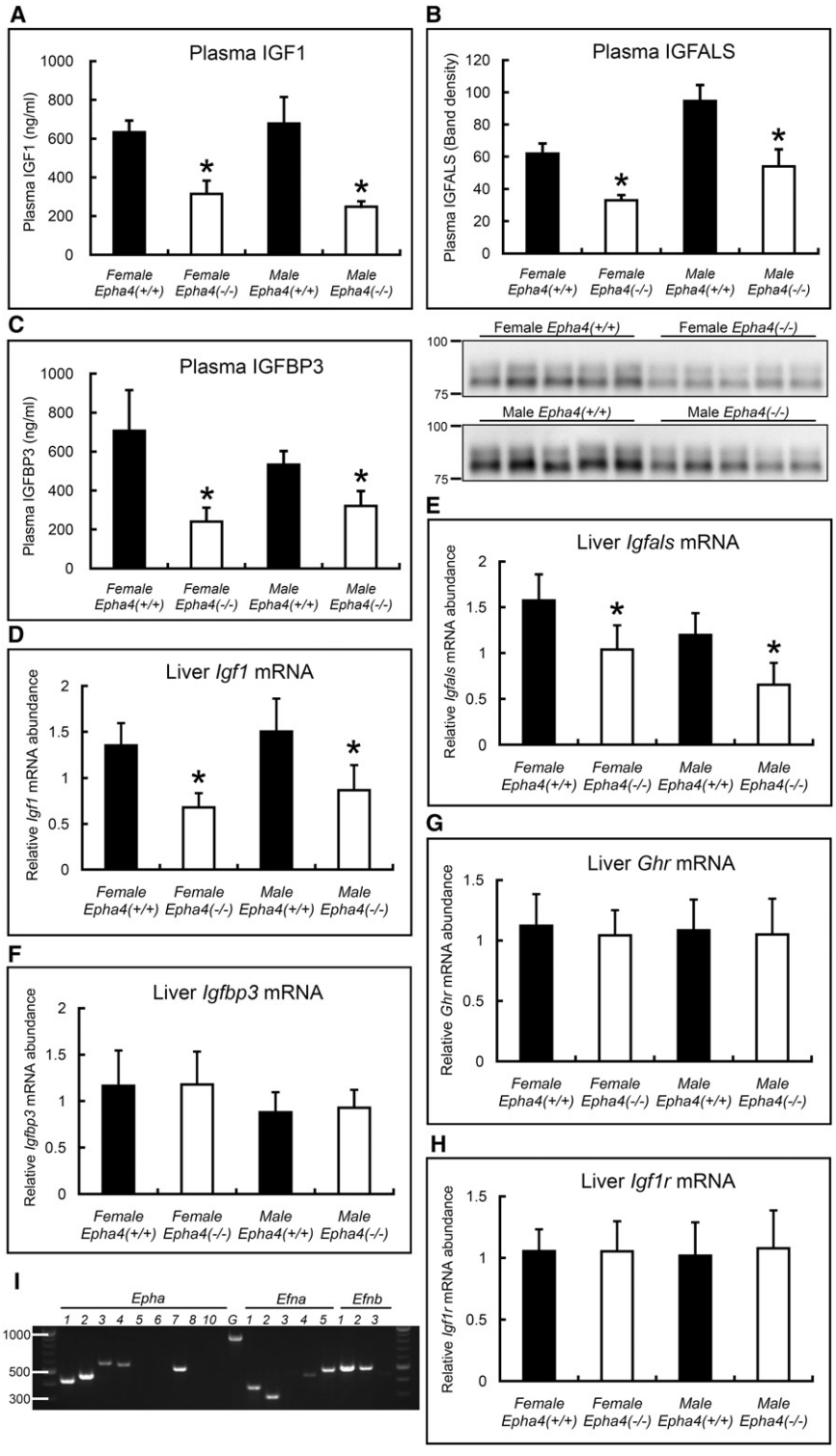

Figure 2. Circulating Levels of IGF1, IGFALS, and IGFBP3 and Hepatic mRNA Expression of *Igf1, Igfals, Igfbp3, Ghr, Igf1r, Epha*s, and *Efn*s

(A–H) Plasma values of IGF1 (A), IGFALS (B), and IGFBP3 (C) in *Epha4*-targeted mice. Plasma concentrations of IGF1 and IGFBP3 were measured using ELISA kits. Relative plasma IGFALS levels were determined by immunoblotting of plasma samples (bottom panel of B), followed by a densitometric analysis (B, top panel). Expression of liver *Igf1* mRNA (D), *Igfals* mRNA (E), *Igfbp3* mRNA (F), *Ghr* mRNA (G), and *Igf1r* mRNA (H) in the *Epha4*-targeted mice. Quantitative real-time RT-PCR was carried out as described, and relative *Igf1* mRNA abundance was calculated according to the comparative Ct (delta delta Ct) method, using *Gapdh* mRNA as a control. Data in (A)–(H) are presented as mean ± SD values of eight independent samples. *p < 0.01 compared with *Epha4*$^{+/+}$ mice of the same sex.

(I) Expression of mRNA for the families of *Epha, Efna,* and *Efnb* in the liver. RT-PCR was performed as described. *G*, *Gapdh* mRNA.

See also Figure S1.

To further clarify the direct interaction between EphA4 and GHR, we carried out binding studies in *Jak2*$^{-/-}$ fibroblasts (Wagner et al., 2004) (Figure 4G). Results showed that EphA4 bound to GHR in the absence of JAK2, supporting the results of Figure 4A. In addition, binding of EphA4 to GHR was enhanced by preincubation of *Jak2*$^{-/-}$ fibroblasts with ephrin-A1 or GH.

Effect of EphA4 Expression on *Igf1* mRNA Expression in Fibroblasts

We examined how rescued expression of EphA4 affected expression of *Igf1* mRNA in *Epha4*$^{-/-}$ fibroblasts (Figure 4H). Fibroblasts with rescued EphA4 expression showed enhanced basal *Igf1* mRNA expression and augmented response to GH or ephrin-A1 compared with control fibroblasts transduced with vector alone. These findings suggested that EphA4 was not only an important molecular component of the GH signaling pathway, but was also related to GH-independent *Igf1* mRNA expression (basal expression level of *Igf1* mRNA).

phosphorylation of GHR-bound tyrosine-containing molecules, including EphA4 and JAK2, in EphA4-rescued cells, followed by weak STAT5B phosphorylation at a later time point (120 min), whereas STAT5B phosphorylation was not present in non-rescued cells (Figure 4F).

We further examined whether the effect of EphA4 was mediated by JAK2 in *Jak2*$^{-/-}$ fibroblasts with or without rescued *Jak2*, which express endogenous EphA4 or overexpress it. In cells transduced with retrovirus vector carrying *Jak2* and/or *EphA4* expression cassettes, these genes were overexpressed

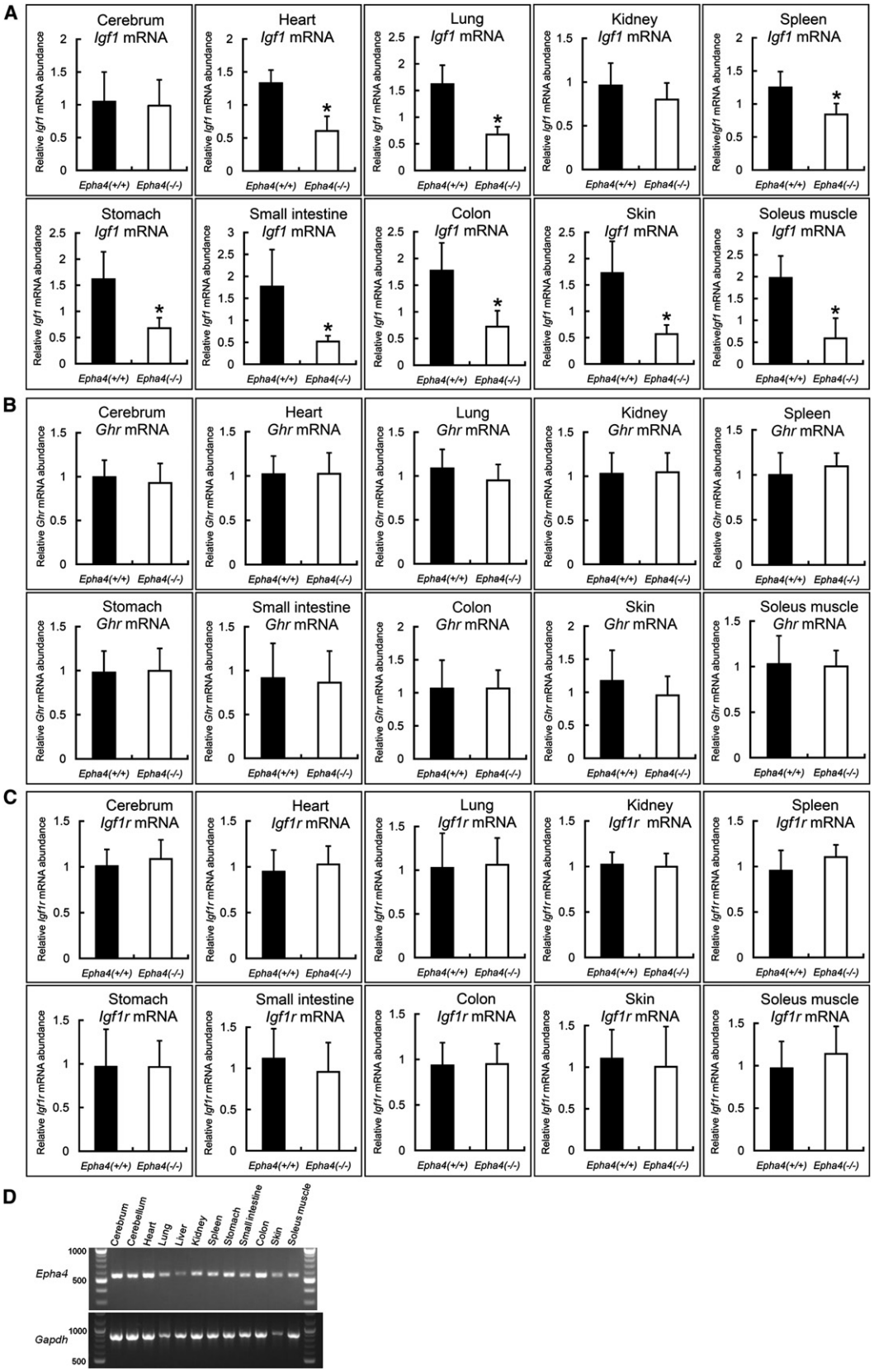
A
Cerebrum Igf1 mRNA
Heart Igf1 mRNA
Lung Igf1 mRNA
Kidney Igf1 mRNA
Spleen Igf1 mRNA
Stomach Igf1 mRNA
Small intestine Igf1 mRNA
Colon Igf1 mRNA
Skin Igf1 mRNA
Soleus muscle Igf1 mRNA
Relative Igf1 mRNA abundance
Epha4(+/+) Epha4(-/-)
B
Cerebrum Ghr mRNA
Heart Ghr mRNA
Lung Ghr mRNA
Kidney Ghr mRNA
Spleen Ghr mRNA
Stomach Ghr mRNA
Small intestine Ghr mRNA
Colon Ghr mRNA
Skin Ghr mRNA
Soleus muscle Ghr mRNA
Relative Ghr mRNA abundance
C
Cerebrum Igf1r mRNA
Heart Igf1r mRNA
Lung Igf1r mRNA
Kidney Igf1r mRNA
Spleen Igf1r mRNA
Stomach Igf1r mRNA
Small intestine Igf1r mRNA
Colon Igf1r mRNA
Skin Igf1r mRNA
Soleus muscle Igf1r mRNA
Relative Igf1r mRNA abundance
D
Cerebrum
Cerebellum
Heart
Lung
Liver
Kidney
Spleen
Stomach
Small intestine
Colon
Skin
Soleus muscle
Epha4
Gapdh
1000
500

and the products were phosphorylated slightly, suggesting a primed active state of these receptors (Figure 5A). In the absence of stimulation with ephrin-A1, STAT5B was phosphorylated only in *Jak2*-rescued cells, with a large enhancement by EphA4 overexpression. Corresponding to these results, the *Igf1* mRNA expression level increased when *Jak2* was rescued and the increase became significant when EphA4 was overexpressed (Figure 5B).

In these cells, ephrin-A1 induced STAT5B phosphorylation in the presence of JAK2 expression, with a peak at approximately 60 min to 120 min of exposure (Figure 5C). Surprisingly, STAT5B was also phosphorylated in *Jak2*$^{-/-}$ fibroblasts, and its phosphorylation was enhanced by overexpressed EphA4, suggesting the presence of a JAK2-independent STAT5B activation pathway mediated by EphA4. As shown at the bottom of Figure 5C, STAT5B was coimmunoprecipitated with EphA4 only before stimulation with ephrin-A1 (at 0 min points), even in the absence of JAK2, suggesting a direct complex formation of nonphosphorylated STAT5B with EphA4 and a quick release of phosphorylated STAT5B from the complex. These findings are in agreement with those shown in Figure 4B.

In accordance with these results, in the presence of endogenous EphA4 expression, *Igf1* mRNA expression increased greatly in response to ephrin-A1 when *Jak2* was rescued (Figure 5D), implying ephrin-A1-mediated augmentation of *Igf1* transcription in the presence of primed JAK2 activation. To examine whether the effect of ephrin/Eph signal was mediated totally by JAK2, we also tested the effect of ephrin-A1 on *Igf1* expression in *Jak2*$^{-/-}$ cells with varying expression levels of EphA4 (Figure 5E). The *Igf1* mRNA expression increased significantly beyond the unstimulated basal level, although the response was almost one-tenth that of the *Jak2*-rescued cells. In the presence of rescued *Jak2* expression, EphA4 overexpression alone increased the basal *Igf1* mRNA expression level and ephrin-A1 treatment further increased this expression (Figure 5F). Taken together, in an ephrin ligand-activated state, 90% of the effect of EphA4 was mediated by JAK2 and 10% appeared to be JAK2-independent in fibroblasts.

Effect of EphA4 on IGF1 Signal Transduction

We also examined signals downstream of IGF1R, insulin receptor substrate 1 (IRS1), MAPK, and AKT in response to varying doses of IGF1 (Figures 6A and 6B). In the absence of preincubation with ephrin-A1, IGF1 induced phosphorylation of IRS1, AKT, and MAPK to a similar level regardless of EphA4 expression (Figure 6B). However, when preincubated with ephrin-A1, IGF1-induced phosphorylation of IRS1, and AKT, a downstream signaling molecule of PI-3 kinase was augmented in *Epha4*$^{-/-}$ cells compared with that in the *EphA4*-rescued cells (Figures 6A and 6C). On the contrary, activity of another signaling molecule, MAPK, was not affected by EphA4 expression or preincubation with ephrin-A1. These findings suggested that the PI-3 kinase pathway downstream of IGF1 signaling was a target signal transduction pathway affected by expression and activation of EphA4.

Effect of Treatment with GH and IGF1

To determine whether IGF1 or GH treatment can recover *Epha4*$^{-/-}$ mice from growth retardation, we subcutaneously injected recombinant human IGF1 (5 mg/kg body weight (BW)/day) or porcine GH (10 mg/kgBW/day) into female mice between 6 and 10 weeks of age (Figures 7A–7C). The mice treated with IGF1 gained significant weight compared with control mice injected with saline alone and attained the same body size as WT mice after 5 weeks of injections. However, the mice treated with GH did not significantly increase their body weight compared with the control mice. Consistent with this finding, plasma IGF1 level did not change in response to GH treatment (Figure 7D).

DISCUSSION

We have presented evidence that EphA4 is an important component of the GHR signaling pathway, leading to IGF1 synthesis without affecting the expression of GHR or IGF1R. It has been reported that JAK2/STAT5B mediates the expression of *IGF1* mRNA after GH-mediated activation of GHR (Piwien-Pilipuk et al., 2002). In the present study, we demonstrated that interaction of EphA4 with GHR, JAK2, and STAT5B resulted in enhanced JAK2/STAT5B activation in response to stimulation with ephrin and GH, leading to enhancement of JAK2/STAT5B-dependent *Igf1* mRNA expression. For this signal activation in fibroblasts, GH plays a major role. In addition, another signal leading to increased *Igf1* mRNA expression can be induced without JAK2 (JAK2 independent) and is dependent on activation of EphA4 by its ligand, ephrin. STAT5B directly binds to EphA4 and mediates this JAK2-independent *Igf1* expression. The significance of this EphA4/STAT5B signaling pathway remains to be elucidated, given that the extent of *Igf1* mRNA production by this pathway is weak in fibroblasts. Because endogenous ephrin is not circulating, it should function in a cell-cell contact-mediated fashion. We have preliminary binding data, obtained by using deletion mutants of EphA4, which show that GHR binds to the extracellular domain of EphA4 and that EphA4 contains the binding site for STAT5B (D.A., T.S., and K.S., unpublished data). There is one report that the JAK2 and STAT proteins are downstream targets of EphA4 signaling in the regulation of muscle acetylcholinesterase expression (Lai et al., 2004). This might be explained by our finding that EphA4, GHR, and JAK2 form a complex. We have also shown

Figure 3. Extrahepatic Expression of mRNAs for *Igf1*, *Ghr*, *Igf1r*, and *Epha4*

(A–C) Expression of *Igf1* mRNA (A), *Ghr* mRNA (B), and *Igf1r* mRNA (C) in various tissues. Tissue RNA was extracted from cerebrum (female), heart (female), lung (male), kidney (male), spleen (female), stomach (female), small intestine (female), colon (female), skin (male), and soleus muscle (male), and quantitative real-time PCR was carried out as described. Data in (A)–(C) are presented as mean ± SD values of eight independent samples from the same sex and are similar for both sexes. *$p < 0.01$ compared with *Epha4*$^{+/+}$ mice.

(D) Expression of *Epha4* in various tissues. RT-PCR was performed as described.

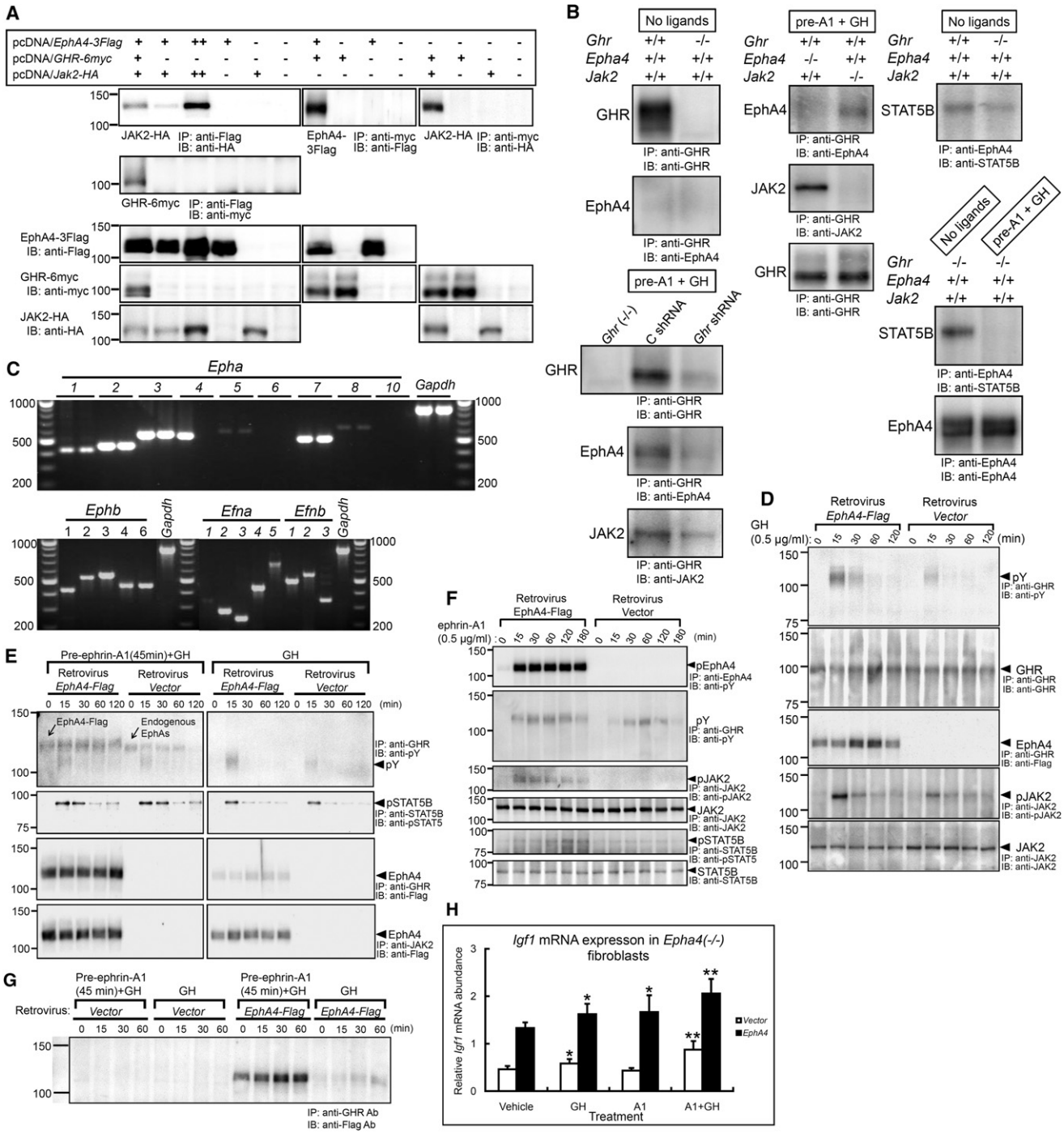

Figure 4. Interaction of EphA4, GHR, and JAK2 and Signaling via the Complex

(A) Interaction of EphA4, GHR, and JAK2 in HEK293T cells. *EphA4-3Flag, GHR-6myc,* and *Jak2-HA* in pcDNA3.1 vector were expressed in HEK293T cells, and their interaction was studied via immunoprecipitation (IP) and/or immunoblotting (IB).

(B) Interaction of endogenous EphA4, GHR, and JAK2 in mouse fibroblasts. Fibroblasts derived from *Epha4*$^{-/-}$, *Jak2*$^{-/-}$, *Ghr*$^{-/-}$, and WT mice were preincubated with serum-free medium overnight (no ligands) and incubated with ephrin-A1 for 45 min followed by treatment with GH for 30 min (pre-A1 + GH). Cell lysates were used for IP and/or IB studies with the indicated antibodies. The WT fibroblasts were also infected with a lentivirus that expressed *Ghr* shRNAs or with a control shRNA (*C* shRNA).

(C) RT-PCR of *Epha* (upper panel), *Ephb*, *Efna*, and *Efnb* (bottom panel) families of mRNAs. Except for *Epha4*, all *Eph* and *Efn* expression levels were comparable in *Epha4*$^{-/-}$ (right lanes) and retrovirally *Epha4*-rescued (left lanes) mouse fibroblasts, although only *Epha* family mRNAs are shown for these two origins of fibroblasts (upper panel). The same amount of RNA from each sample was used for RT.

that EphA4 does not alter IGF1/IGF1R-mediated MAPK activity, but merely desensitizes the response of the PI-3 kinase pathway upon activation with ephrin, making it difficult to attribute the growth retardation in *Epha4*-knockout mice to the derangement of IGF1R-EphA4 interaction. We speculate that the lack or loss of EphA4 signaling, possibly due to mutations or polymorphisms of *EphA4*, causes deficient IGF1 synthesis via suppression of both the GHR/EphA4/JAK2/STAT5B and the EphA4/STAT5B pathways, leading to growth retardation.

The present findings that *Epha4*-knockout mice exhibited short stature with low circulating levels of IGF1, IGFALS, and IGFBP3 and low *Igf1* mRNA expression in many tissues are consistent with the idea that IGF1 of both endocrine and local origin plays an important role in body growth. In a study in mice lacking *Ghr* and/or *Igf1* (Lupu et al., 2001) and another study in mice carrying liver-specific expression of *Igf1* via cognate *Igf1* promoters in an *Igf1* null background (Stratikopoulos et al., 2008), their results showed that endocrine IGF1 indeed significantly contributes (30%) to adult body size with a 39% contribution of local tissue IGF1. In *Epha4*-knockout mice, levels of plasma IGF1, IGFALS, and IGFBP3 were one-third to one-half those of WT mice. These levels are not as low as those in the conditional hepatic *Igf1*-knockout mice (Sjögren et al., 1999; Yakar et al., 1999) that show normal body size. Nevertheless, *Epha4*-knockout mice exhibited short stature. This discrepancy may be explained by congenital deletion of EphA4 from both the liver and local tissues in *Epha4*-knockout mice and gradual postnatal deletion of *Igf1* expression from the liver in the hepatic *Igf1*-knockout mice. Furthermore, our results, which show that IGF1 but not GH replacement treatment is effective for restoring body growth, are compatible with the derangement of GHR signal transduction in *Epha4*-knockout mice. This finding supports the notion that endocrine IGF1 plays an important role in normal body growth.

The *Epha4*-knockout mice showed deranged expression of local *Igf1* in many tissues. This local *Igf1* expression does not completely depend on GH in all tissues (Lupu et al., 2001). Expression of *Igf1* in tissues, such as the skeletal system, brain, lung, heart, spleen, testis, and uterus, appears to be GH-independent, and the expression depends in part on GH in skeletal muscle, adipose tissue, ovary, and kidney, in contrast to the complete dependence on GH in the liver. In the present study, *Epha4*-knockout mice showed a significantly decreased amount of *Igf1* mRNA compared with WT mice in many tissues, including lung, heart, and spleen. These tissues likely depend heavily on EphA4 for *Igf1* expression. However, cerebrum and kidney showed no significant decrease in *Igf1* mRNA, suggesting that EphAs other than EphA4 might compensate for the function of EphA4 in these tissues. Alternatively, the function of EphA4 might be less important than other signals for IGF1 expression in some tissues, including brain and kidney.

The plasma GH level was unaltered in *Epha4*-knockout mice. The reason for the unchanged plasma GH level, which could be elevated in the presence of a low plasma IGF1 level, remains to be clarified. Since neither *Gh* mRNA expression in the pituitary nor *Igf1r* mRNA expression in other tissues was altered, the plasma levels of IGF1 (35%–50% of WT mice) might not be low enough to induce GH synthesis or secretion. The apparent low levels of plasma IGF1 might also be exaggerated by low levels of IGFBP3 and IGFALS in *Epha4*-knockout mice. IGFBP3 and IGFALS are important counterparts for ternary complex formation with IGF1 in the circulation and determinants of circulating IGF1 concentration (Binoux, 1997). In mice with a liver-specific *Igf1* gene deletion or a double deletion of liver *Igf1* and *Igfals* genes, GH level is elevated due to loss of feedback suppression by low levels of serum IGF1 (Sjögren et al., 1999; Yakar et al., 1999, 2006). However, mice with single genetic deletion of *Igfals* or *Igfbp3* do not show such increases in serum GH level, despite a significant reduction in serum IGF1 level (Yakar et al., 2006, 2009). These findings suggest that the formation of a ternary complex of IGF1 with IGFBP3 and IGFALS does not constitute the functional fraction of IGF1, which is not clearly defined at this moment in the feedback mechanism of GH synthesis or secretion (Elis et al., 2011). In the case of *Epha4*-knockout mice in which liver *Igfbp3* expression is kept normal and expression of both *Igf1* and *Igfals* is low, the IGF1 fraction responsible for GH suppression might not be reduced, despite the reduced total plasma IGF1 level. Another possibility is that this discrepancy might be caused by derangement of the feedback signaling mechanism from IGF1 to GH, owing to absence of EphA4 in the pituitary and/or hypothalamus (Giustina and Veldhuis, 1998). The feedback mechanism in somatotroph cells appears to be mediated by PI-3 kinase, not by MAPK or S6 kinase (Niiori-Onishi et al., 1999). In our study, deletion of *Epha4* in fibroblasts clearly sensitized activation of AKT, a downstream signaling molecule of PI-3 kinase, after

(D) Effect of GH on the GHR/JAK2 signal. *Epha4*$^{-/-}$ (retrovirus vector) and *Epha4*-rescued (retrovirus *EphA4-Flag*) fibroblasts were incubated with GH for the time periods shown at the top. Samples were immunoprecipitated and detected by immunoblotting with the indicated antibodies. pY, phosphorylated tyrosine.
(E) (Top four panels) Effect of activation of Eph receptors and/or GHR by ligands on the tyrosine phosphorylation of GHR/JAK2 and STAT5B. *Epha4*$^{-/-}$ and *Epha4*-rescued fibroblasts were incubated with GH for the time periods shown at the top with or without a 45 min preincubation with ephrin-A1 (pre-ephrin-A1). Samples were immunoprecipitated and detected by immunoblotting with the indicated antibodies. (Bottom four panels) Interaction of EphA4 with GHR and JAK2. Study conditions were identical in the four groups of samples detected by the same antibodies.
(F) Effect of ephrin-A1 on GHR/JAK2/STAT5B phosphorylation. *Epha4*$^{-/-}$ and *Epha4*-rescued fibroblasts were incubated with ephrin-A1 for the time periods shown at the top. Samples were detected by immunoblotting with or without immunoprecipitation using the indicated antibodies.
(G) Interaction of endogenous GHR with EphA4 in the absence of JAK2 expression. *EphA4-Flag*-overexpressing *Jak2*$^{-/-}$ fibroblasts were incubated with GH for the time periods shown at the top with or without pre-ephrin-A1treatment for 45 min. Interaction of GHR with EphA4-Flag was detected by immunoblotting following immunoprecipitation using the indicated antibodies.
(H) Effect of ligand stimulation on *Igf1* mRNA expression in *Epha4*$^{-/-}$ (white bars) and *Epha4*-rescued (black bars) fibroblasts. Fibroblasts were incubated with GH and/or ephrin-A1 for 36 hr. Data are presented as mean ± SD values of six independent experiments. *$p < 0.05$ and **$p < 0.01$ compared with the vehicle-treated cells.
See also Figures S1 and S2.

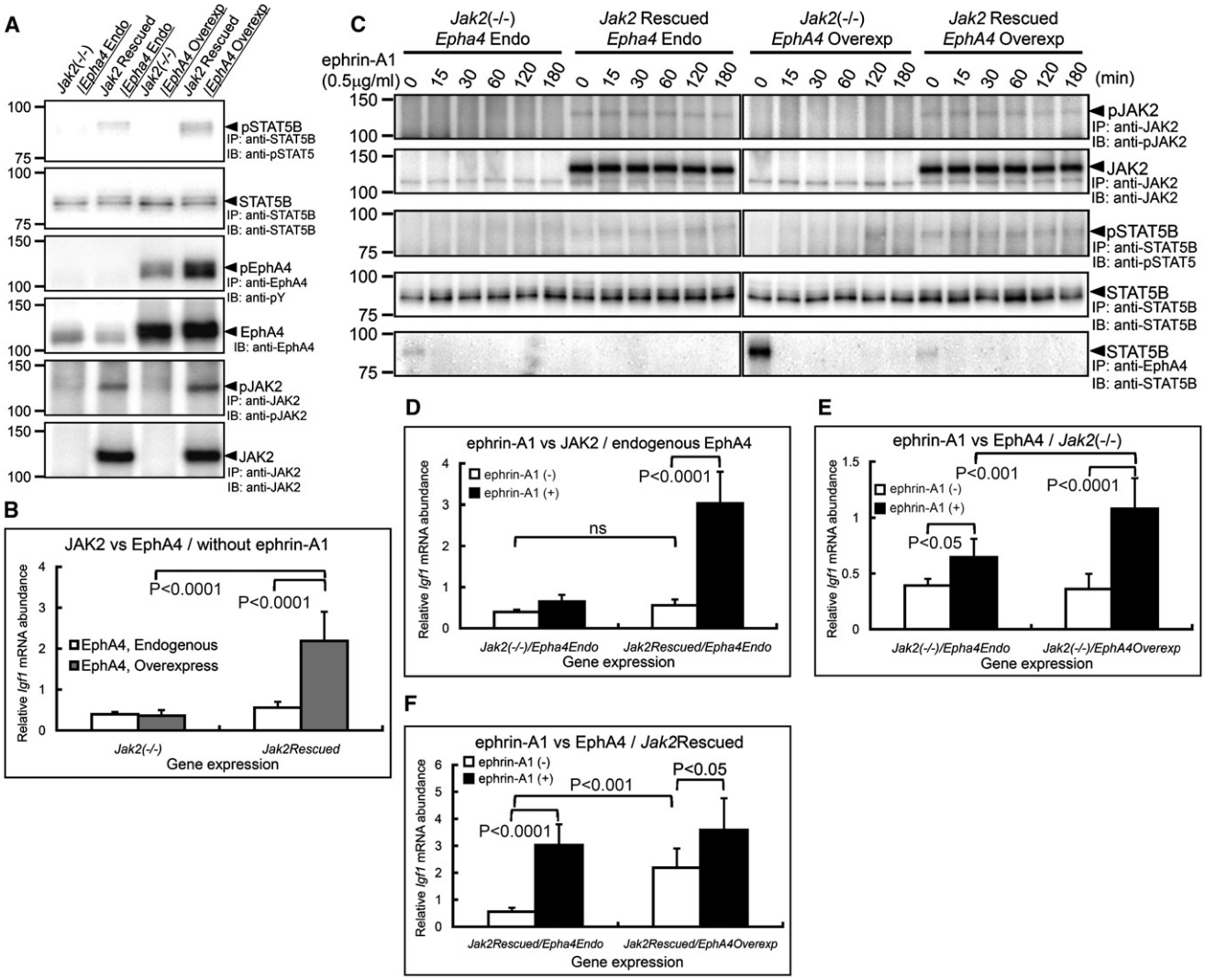

Figure 5. Effect of *EphA4* or *Jak2* Expression and Ephrin-A1 Stimulation on *Igf1* mRNA Expression in *Jak2*$^{-/-}$ Fibroblasts

(A) Basal expression of pSTAT5B, STAT5B, pEphA4, EphA4, pJAK2, and JAK2 in *Jak2*$^{-/-}$ and *Jak2*-rescued fibroblasts with or without *EphA4* overexpression. Cell lysates were immunoprecipitated and immunoblotted with the indicated antibodies.

(B) Effect of EphA4 overexpression (gray bars) on *Igf1* mRNA expression in *Jak2*$^{-/-}$ and *Jak2*-rescued fibroblasts. Cells expressing endogenous *Epha4* are indicated by white bars.

(C) Effect of ephrin-A1 on the phosphorylation of JAK2 and STAT5B and on the binding of STAT5B to the complex involving EphA4 in *Jak2*$^{-/-}$ and *Jak2*-rescued fibroblasts with or without *EphA4* overexpression. Cells were exposed to ephrin-A1 for the time periods shown. Cell lysates were subjected to immunoprecipitation and immunoblotting with the indicated antibodies. Endo, endogenous; Overexp, overexpressed.

(D) Effect of ephrin-A1 stimulation (black bars) and/or *Jak2* expression rescue on *Igf1* mRNA expression in *Jak2*$^{-/-}$ fibroblasts expressing endogenous *Epha4*. Cells not stimulated with ephrin-A1 are indicated by white bars hereafter.

(E) Effect of ephrin-A1 stimulation (black bars) and/or EphA4 overexpression on *Igf1* mRNA expression in *Jak2*$^{-/-}$ fibroblasts.

(F) Effect of ephrin-A1 stimulation and/or EphA4 overexpression on *Igf1* mRNA expression in *Jak2*-rescued fibroblasts.

Data in (B), (D), (E), and (F) are presented as mean ± SD values of six independent experiments. Statistical analysis was carried out via two-way ANOVA followed by the Neuman-Keuls multiple comparison test.

IGF1 stimulation in the presence of ephrin-A1 pretreatment. This might explain, at least partially, the discrepancy shown here if the same mechanism is applicable to somatotroph cells in the pituitary gland.

In conclusion, we have demonstrated that EphA4 plays an important role in JAK2-dependent and -independent signal transduction pathways, leading to increased IGF1 production. The absence of EphA4 expression decreased the amount of IGF1 in the circulation and locally in tissues, which contributed to the short stature. Our results propose a model in which a long-range GH/GHR-mediated humoral signal is modulated by a short-range, cell-cell contact-mediated ephrin/Eph signal for determining body and organ size. This finding implies the presence of a fine-tuning mechanism for appropriate body and

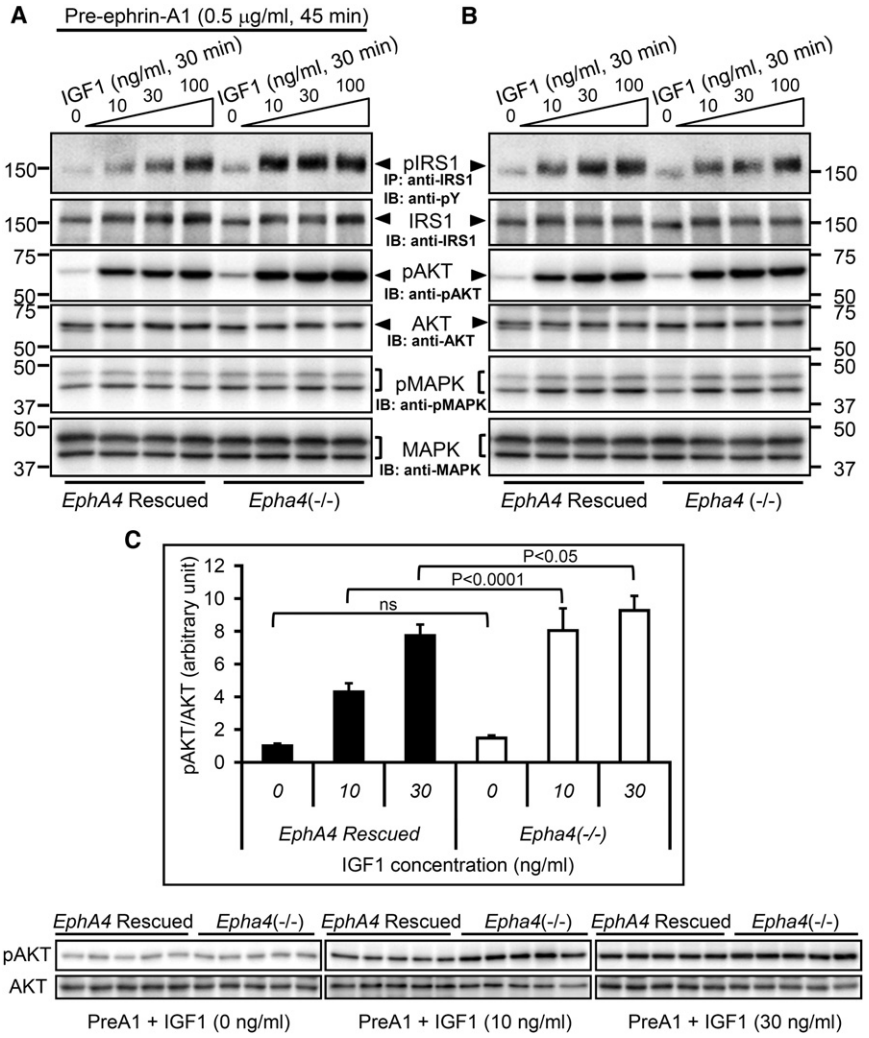

Figure 6. IGF1 Signaling in the Presence or Absence of EphA4 Expression

Epha4$^{-/-}$ and *EphA4*-rescued fibroblasts were incubated for 30 min with IGF1 in the presence (A) or absence (B) of preincubation with ephrin-A1 for 45 min. Activation of IRS1, AKT, and MAPK were examined with antibodies that detect active phosphorylated molecules (pIRS1, pAKT, and pMAPK) and total amount of these proteins (IRS1, AKT, and MAPK).

(C) Effect of ephrin-A1 preincubation (PreA1) on AKT activation. AKT activation after a 30 min IGF1 stimulation was quantified in five different experiments (bottom blotting data), and values were expressed as the ratio of pAKT/AKT (top graph). ns, not significantly different.

organ size that is coordinated by both humoral factors and local cell-cell interactions through a shared signaling pathway.

EXPERIMENTAL PROCEDURES

Animals

All animal experiments were performed in compliance with the guidelines of the institutional animal committee and the Japanese government.

Epha4-targeted mice were originally obtained from the laboratory of Dr. P. Charnay (Helmbacher et al., 2000). In the current study, data were obtained from the mice of a mixed background that were maintained in a closed colony, as described in the Extended Experimental Procedures. Littermate controls were used for histological and morphological studies, and for other studies, mice of different genotypes in the closed colony were used for comparison.

Mice between 6 and 10 weeks were used for treatment with human IGF1 and porcine GH. IGF1 (5 mg/kgBW/day) or GH (10 mg/kgBW/day) dissolved in saline was subcutaneously injected into mice once a day at 9 a.m. Body weight was measured once a week for 5 weeks.

Measurements of Body Weight, Body Length, and Food Intake

Starting from birth, body weights of all mice were measured weekly for 28 weeks with a calibrated electronic balance (SP601 Scout Pro Balance; Ohaus Corp.).

Body length (nose-to-anus distance) was measured at 16 weeks or older with an electronic digital caliper (Traceable Digital Caliper; Fisher Scientific). Food intake was measured daily as the weight difference of dried food in the cage. Scattered food was carefully collected for weighing.

Assays of Plasma GH, Thyroxine, and Corticosterone

Mice were killed by decapitation in the morning, and blood was collected in a tube with a drop of heparin for separation of plasma by centrifugation. Growth hormone was measured with a rat/mouse growth hormone 96-well plate assay kit (Millipore; catalog #EZRMGH-45K), thyroxine was measured by SRL (Tokyo, Japan) with the use of a Cobas T4 assay system, and corticosterone was measured by SRL according to a reported method (Nabors et al., 1974).

Assays of Plasma IGF1 and IGFBP3

Plasma levels of IGF1 and IGFBP3 were measured with a mouse IGF1 HS Elisa Kit (Immunodiagnostic Systems Ltd.) and a Duoset Elisa Development Kit for mouse IGFBP3 (R&D Systems), respectively, according to manufacturers' instructions.

Cells

Mouse fibroblasts with genotypes of WT, *Epha4*$^{-/-}$, and *Ghr*$^{-/-}$ (Zhou et al., 1997) were derived from E14.5 mice using a standard protocol, and the genotype was determined subsequently. Cells from each embryo were maintained individually in Dulbecco's modified Eagle medium (DMEM) supplemented with 10% fetal calf serum. Fibroblasts from *Jak2*$^{-/-}$ mice were a gift from Drs. Wagner and Lin, Nebraska Medical Center. Before incubation with human GH or clustered ephrin-A1, cells were plated onto 6-cm plates at 5 × 10^5 cells per plate, and once at 70% to 80% confluency, they were preincubated overnight with serum-free minimum essential medium containing 0.5% bovine serum albumin. For quantification of mRNA by real-time RT-PCR, incubation with ligands was usually for 36 hr. For knockdown of *Ghr* mRNA, fibroblasts were infected with a lentivirus expressing shRNAs (Santa Cruz, catalog #sc-40016-v) for *Ghr* mRNA at a multiplicity of infection (MOI) of 10. A control shRNA lentivirus (Santa Cruz, catalog #sc-108080) was also used for control cells with the same MOI.

HEK293T cells were cultured and used for transfection as described (Sawada et al., 2010). HepG2 cells were provided by the RIKEN BRC through the National Bio-Resource Project of the MEXT, Japan and cultured in DMEM supplemented with 10% fetal calf serum.

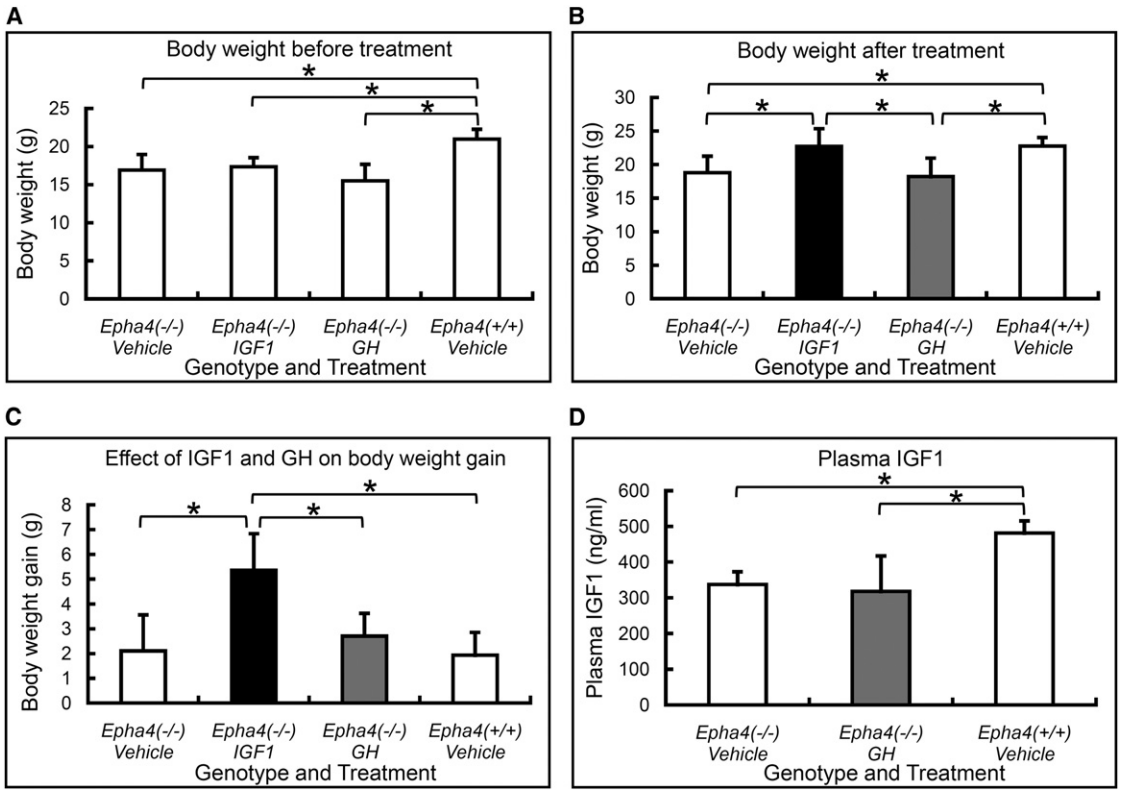

Figure 7. Effect of GH and IGF1 on Body Growth

Mice were treated with IGF1 (5 mg/kgBW) and GH (10 mg/kgBW), and their body weight (A and B), body weight gain (C), and plasma IGF1 levels (D) were measured. Reagent in saline or saline alone was subcutaneously injected into female *Epha4*$^{-/-}$ or *Epha4*$^{+/+}$ mice between 6 and 10 weeks of age once a day, and body weight was compared before and after 5 weeks of treatment. Plasma IGF1 levels were also measured after 5 weeks of treatment and represent only mouse IGF1. Data in each group are presented as mean ± SD values of six independent samples. Data were analyzed statistically by one-way ANOVA followed by the Neuman-Keuls multiple comparison test. *$p < 0.05$.

Construction of Eukaryotic Expression Vectors and Retrovirus Expression Vectors

For transient eukaryotic expression in HEK293T cells, complementary DNAs (cDNAs) for human *EphA4*, mouse *Jak2*, and rabbit *GHR* were incorporated into pcDNA3.1 vector with tags (*3Flag*, *HA*, and *6myc*, respectively). For retroviral expression, cDNA for WT *Epha4* or *Jak2* was ligated into the pMXs-IG vector (Kitamura et al., 2003) and incorporated into retrovirus as reported (Yokote et al., 2005) using cotransfection of the pMXs-IG–based constructs with pCAGVSV-G, which encodes vesicular stomatitis virus surface protein under the control of the chicken β-actin promoter. Transduction of cells with retrovirus was generally performed with a MOI of 5.

Immunoprecipitation and Immunoblotting

Immunoprecipitation and immunoblotting were performed as reported (Yokote et al., 2005; Zhang et al., 2007) according to the standard procedures described in detail in the Extended Experimental Procedures.

RT-PCR

RNA extraction and RT-PCR were carried out according to the standard procedures described in detail in the Extended Experimental Procedures. See also Table S2 for the primers used.

Quantitative Real-Time RT-PCR Analysis

The analysis was carried out according to the standard procedures, as described in the Extended Experimental Procedures. Pituitary *Gh* mRNA was quantified as reported (Iida et al., 2004). To assess expression levels of *Igf1*, *Igfals*, *Igfbp3*, *Ghr*, and *Igf1r* mRNA in tissues and fibroblasts, we used the comparative Ct (delta delta Ct) method to normalize target gene mRNA to *Gapdh* mRNA, as reported (Kohsaka et al., 2007).

In Situ Hybridization

In situ hybridization was carried out according to the standard procedure, as described in the Extended Experimental Procedures. Antisense and sense complementary RNA probes for collagen type II (*Col2a1*; 138–551 of NM031163) were used to identify differentiated chondrocytes. Probes were labeled with digoxigenin (DIG) by a DIG RNA-labeling method (Roche Diagnostics; catalog #1175025) according to the manufacturer's instructions. Samples were examined with a Keyence BZ-9000 microscope.

Statistical Analysis

Comparison between two values was performed by Student's t test. Multiple values were compared by one-way or two-way analysis of variance (ANOVA), depending on the number of variables to be tested, followed by Newman-Keuls multiple comparison test.

SUPPLEMENTAL INFORMATION

Supplemental Information includes Extended Experimental Procedures, two figures, and two tables and can be found with this article online at http://dx.doi.org/10.1016/j.celrep.2012.08.021.

LICENSING INFORMATION

ACKNOWLEDGMENTS

This work was supported in part by a Grant-in-Aid for Scientific Research from the Japanese government (#21591183 and #24591370) and a Research Grant on Priority Areas from Wakayama Medical University. None of the authors have any financial conflict of interest related to this work. Fibroblasts derived from *Jak2*-targeted mice were kindly provided by Drs. Wagner and Lin of the Nebraska Medical Center; Rabbit *GHR* cDNA by Dr. R. Fukunaga of Osaka University; mouse *Jak2* cDNA by Dr. A. Yoshimura of Kyushu University; and *Ghr*-targeted mice by Dr. John J. Kopchick, Ohio University.

K.S. designed the study and wrote the manuscript. X.J. performed genotyping, RT-PCR, quantitative real-time RT-PCR, immunocytochemistry, and in situ hybridization in collaboration with Q.C. and K.F. M.M. maintained mice and performed growth curve studies, food intake studies, and hormonal assays. T.S. and D.A. carried out construction of retrovirus vectors, transfection, and immunoblotting with help from Ms. Emi Shimada and Ms. M. Sakiyama. K.I. and K.C. performed quantitative *Gh* mRNA RT-PCR. Tissue and blood samples were collected by all authors.

Received: October 6, 2011
Revised: July 13, 2012
Accepted: August 20, 2012
Published online: September 20, 2012

REFERENCES

Amselem, S., Duquesnoy, P., Attree, O., Novelli, G., Bousnina, S., Postel-Vinay, M.C., and Goossens, M. (1989). Laron dwarfism and mutations of the growth hormone-receptor gene. N. Engl. J. Med. *321*, 989–995.

Binoux, M. (1997). GH, IGFs, IGF-binding protein-3 and acid-labile subunit: what is the pecking order? Eur. J. Endocrinol. *137*, 605–609.

Birzniece, V., Sata, A., and Ho, K.K. (2009). Growth hormone receptor modulators. Rev. Endocr. Metab. Disord. *10*, 145–156.

Cunningham, B.C., Ultsch, M., De Vos, A.M., Mulkerrin, M.G., Clauser, K.R., and Wells, J.A. (1991). Dimerization of the extracellular domain of the human growth hormone receptor by a single hormone molecule. Science *254*, 821–825.

Domené, H.M., Bengolea, S.V., Martínez, A.S., Ropelato, M.G., Pennisi, P., Scaglia, P., Heinrich, J.J., and Jasper, H.G. (2004). Deficiency of the circulating insulin-like growth factor system associated with inactivation of the acid-labile subunit gene. N. Engl. J. Med. *350*, 570–577.

Elis, S., Wu, Y., Courtland, H.W., Cannata, D., Sun, H., Beth-On, M., Liu, C., Jasper, H., Domené, H., Karabatas, L., et al. (2011). Unbound (bioavailable) IGF1 enhances somatic growth. Dis. Model Mech. *4*, 649–658.

Giustina, A., and Veldhuis, J.D. (1998). Pathophysiology of the neuroregulation of growth hormone secretion in experimental animals and the human. Endocr. Rev. *19*, 717–797.

Godowski, P.J., Leung, D.W., Meacham, L.R., Galgani, J.P., Hellmiss, R., Keret, R., Rotwein, P.S., Parks, J.S., Laron, Z., and Wood, W.I. (1989). Characterization of the human growth hormone receptor gene and demonstration of a partial gene deletion in two patients with Laron-type dwarfism. Proc. Natl. Acad. Sci. USA *86*, 8083–8087.

Helmbacher, F., Schneider-Maunoury, S., Topilko, P., Tiret, L., and Charnay, P. (2000). Targeting of the EphA4 tyrosine kinase receptor affects dorsal/ventral pathfinding of limb motor axons. Development *127*, 3313–3324.

Iida, K., Del Rincon, J.P., Kim, D.S., Itoh, E., Nass, R., Coschigano, K.T., Kopchick, J.J., and Thorner, M.O. (2004). Tissue-specific regulation of growth hormone (GH) receptor and insulin-like growth factor-I gene expression in the pituitary and liver of GH-deficient (lit/lit) mice and transgenic mice that overexpress bovine GH (bGH) or a bGH antagonist. Endocrinology *145*, 1564–1570.

Kitamura, T., Koshino, Y., Shibata, F., Oki, T., Nakajima, H., Nosaka, T., and Kumagai, H. (2003). Retrovirus-mediated gene transfer and expression cloning: powerful tools in functional genomics. Exp. Hematol. *31*, 1007–1014.

Kofoed, E.M., Hwa, V., Little, B., Woods, K.A., Buckway, C.K., Tsubaki, J., Pratt, K.L., Bezrodnik, L., Jasper, H., Tepper, A., et al. (2003). Growth hormone insensitivity associated with a STAT5b mutation. N. Engl. J. Med. *349*, 1139–1147.

Kohsaka, A., Laposky, A.D., Ramsey, K.M., Estrada, C., Joshu, C., Kobayashi, Y., Turek, F.W., and Bass, J. (2007). High-fat diet disrupts behavioral and molecular circadian rhythms in mice. Cell Metab. *6*, 414–421.

Kullander, K., and Klein, R. (2002). Mechanisms and functions of Eph and ephrin signalling. Nat. Rev. Mol. Cell Biol. *3*, 475–486.

Lai, K.O., Chen, Y., Po, H.M., Lok, K.C., Gong, K., and Ip, N.Y. (2004). Identification of the Jak/Stat proteins as novel downstream targets of EphA4 signaling in muscle: implications in the regulation of acetylcholinesterase expression. J. Biol. Chem. *279*, 13383–13392.

Laron, Z., Pertzelan, A., and Mannheimer, S. (1966). Genetic pituitary dwarfism with high serum concentation of growth hormone—a new inborn error of metabolism? Isr. J. Med. Sci. *2*, 152–155.

Lupu, F., Terwilliger, J.D., Lee, K., Segre, G.V., and Efstratiadis, A. (2001). Roles of growth hormone and insulin-like growth factor 1 in mouse postnatal growth. Dev. Biol. *229*, 141–162.

MacLeod, J.N., Pampori, N.A., and Shapiro, B.H. (1991). Sex differences in the ultradian pattern of plasma growth hormone concentrations in mice. J. Endocrinol. *131*, 395–399.

Nabors, C.J., Jr., West, C.D., Mahajan, D.K., and Tyler, F.H. (1974). Radioimmunoassay of human plasma corticosterone: method, measurement of episodic secretion and adrenal suppression and stimulation. Steroids *23*, 363–378.

Naski, M.C., Colvin, J.S., Coffin, J.D., and Ornitz, D.M. (1998). Repression of hedgehog signaling and BMP4 expression in growth plate cartilage by fibroblast growth factor receptor 3. Development *125*, 4977–4988.

Niiori-Onishi, A., Iwasaki, Y., Mutsuga, N., Oiso, Y., Inoue, K., and Saito, H. (1999). Molecular mechanisms of the negative effect of insulin-like growth factor-I on growth hormone gene expression in MtT/S somatotroph cells. Endocrinology *140*, 344–349.

Ornitz, D.M. (2001). Regulation of chondrocyte growth and differentiation by fibroblast growth factor receptor 3. Novartis Found. Symp. *232*, 63–76, discussion 76–80, 272–282.

Pasquale, E.B. (2008). Eph-ephrin bidirectional signaling in physiology and disease. Cell *133*, 38–52.

Pilecka, I., Whatmore, A., Hooft van Huijsduijnen, R., Destenaves, B., and Clayton, P. (2007). Growth hormone signalling: sprouting links between pathways, human genetics and therapeutic options. Trends Endocrinol. Metab. *18*, 12–18.

Piwien-Pilipuk, G., Huo, J.S., and Schwartz, J. (2002). Growth hormone signal transduction. J. Pediatr. Endocrinol. Metab. *15*, 771–786.

Rowlinson, S.W., Behncken, S.N., Rowland, J.E., Clarkson, R.W., Strasburger, C.J., Wu, Z., Baumbach, W., and Waters, M.J. (1998). Activation of chimeric and full-length growth hormone receptors by growth hormone receptor monoclonal antibodies. A specific conformational change may be required for full-length receptor signaling. J. Biol. Chem. *273*, 5307–5314.

Sawada, T., Jing, X., Zhang, Y., Shimada, E., Yokote, H., Miyajima, M., and Sakaguchi, K. (2010). Ternary complex formation of EphA4, FGFR and FRS2alpha plays an important role in the proliferation of embryonic neural stem/progenitor cells. Genes Cells *15*, 297–311.

Sjögren, K., Liu, J.L., Blad, K., Skrtic, S., Vidal, O., Wallenius, V., LeRoith, D., Törnell, J., Isaksson, O.G., Jansson, J.O., and Ohlsson, C. (1999). Liver-derived insulin-like growth factor I (IGF-I) is the principal source of IGF-I in

blood but is not required for postnatal body growth in mice. Proc. Natl. Acad. Sci. USA *96*, 7088–7092.

Stratikopoulos, E., Szabolcs, M., Dragatsis, I., Klinakis, A., and Efstratiadis, A. (2008). The hormonal action of IGF1 in postnatal mouse growth. Proc. Natl. Acad. Sci. USA *105*, 19378–19383.

Wagner, K.U., Krempler, A., Triplett, A.A., Qi, Y., George, N.M., Zhu, J., and Rui, H. (2004). Impaired alveologenesis and maintenance of secretory mammary epithelial cells in Jak2 conditional knockout mice. Mol. Cell. Biol. *24*, 5510–5520.

Walenkamp, M.J., and Wit, J.M. (2006). Genetic disorders in the growth hormone - insulin-like growth factor-I axis. Horm. Res. *66*, 221–230.

Woods, K. (2007). Genetic defects of the growth-hormone-IGF axis associated with growth hormone insensitivity. Endocr. Dev. *11*, 6–15.

Woods, K.A., Camacho-Hübner, C., Savage, M.O., and Clark, A.J. (1996). Intrauterine growth retardation and postnatal growth failure associated with deletion of the insulin-like growth factor I gene. N. Engl. J. Med. *335*, 1363–1367.

Yakar, S., Liu, J.L., Stannard, B., Butler, A., Accili, D., Sauer, B., and LeRoith, D. (1999). Normal growth and development in the absence of hepatic insulin-like growth factor I. Proc. Natl. Acad. Sci. USA *96*, 7324–7329.

Yakar, S., Bouxsein, M.L., Canalis, E., Sun, H., Glatt, V., Gundberg, C., Cohen, P., Hwang, D., Boisclair, Y., Leroith, D., and Rosen, C.J. (2006). The ternary IGF complex influences postnatal bone acquisition and the skeletal response to intermittent parathyroid hormone. J. Endocrinol. *189*, 289–299.

Yakar, S., Rosen, C.J., Bouxsein, M.L., Sun, H., Mejia, W., Kawashima, Y., Wu, Y., Emerton, K., Williams, V., Jepsen, K., et al. (2009). Serum complexes of insulin-like growth factor-1 modulate skeletal integrity and carbohydrate metabolism. FASEB J. *23*, 709–719.

Yokote, H., Fujita, K., Jing, X., Sawada, T., Liang, S., Yao, L., Yan, X., Zhang, Y., Schlessinger, J., and Sakaguchi, K. (2005). Trans-activation of EphA4 and FGF receptors mediated by direct interactions between their cytoplasmic domains. Proc. Natl. Acad. Sci. USA *102*, 18866–18871.

Zhang, J., and Hughes, S. (2006). Role of the ephrin and Eph receptor tyrosine kinase families in angiogenesis and development of the cardiovascular system. J. Pathol. *208*, 453–461.

Zhang, Y., Sawada, T., Jing, X., Yokote, H., Yan, X., and Sakaguchi, K. (2007). Regulation of ephexin1, a guanine nucleotide exchange factor of Rho family GTPases, by fibroblast growth factor receptor-mediated tyrosine phosphorylation. J. Biol. Chem. *282*, 31103–31112.

Zhou, Y., Xu, B.C., Maheshwari, H.G., He, L., Reed, M., Lozykowski, M., Okada, S., Cataldo, L., Coschigamo, K., Wagner, T.E., et al. (1997). A mammalian model for Laron syndrome produced by targeted disruption of the mouse growth hormone receptor/binding protein gene (the Laron mouse). Proc. Natl. Acad. Sci. USA *94*, 13215–13220.